

RESEARCH BRIEF

A Coding Single-Nucleotide Polymorphism in Lysine Demethylase *KDM4A* Associates with Increased Sensitivity to mTOR Inhibitors

Capucine Van Rechem¹, Joshua C. Black¹, Patricia Greninger¹, Yang Zhao^{2,3}, Carlos Donado¹, Paul d. Burrowes¹, Brendon Ladd¹, David C. Christiani^{2,4}, Cyril H. Benes¹, and Johnathan R. Whetstine¹

ABSTRACT

SNPs occur within chromatin-modulating factors; however, little is known about how these variants within the coding sequence affect cancer progression or treatment. Therefore, there is a need to establish their biochemical and/or molecular contribution, their use in subclassifying patients, and their impact on therapeutic response. In this report, we demonstrate that coding SNP-A482 within the lysine trimethylase gene *KDM4A/JMJD2A* has different allelic frequencies across ethnic populations, associates with differential outcome in patients with non-small cell lung cancer (NSCLC), and promotes *KDM4A* protein turnover. Using an unbiased drug screen against 87 preclinical and clinical compounds, we demonstrate that homozygous SNP-A482 cells have increased mTOR inhibitor sensitivity. mTOR inhibitors significantly reduce SNP-A482 protein levels, which parallels the increased drug sensitivity observed with *KDM4A* depletion. Our data emphasize the importance of using variant status as candidate biomarkers and highlight the importance of studying SNPs in chromatin modifiers to achieve better targeted therapy.

SIGNIFICANCE: This report documents the first coding SNP within a lysine demethylase that associates with worse outcome in patients with NSCLC. We demonstrate that this coding SNP alters the protein turnover and associates with increased mTOR inhibitor sensitivity, which identifies a candidate biomarker for mTOR inhibitor therapy and a therapeutic target for combination therapy. *Cancer Discov*; 5(3); 245-54. ©2015 AACR.

See related commentary by Rothbart et al., p. 228.

See related article by Van Rechem et al., p. 255.

INTRODUCTION

SNPs, the most common type of genetic differences in humans, are defined as a single base-pair difference in the DNA with the least abundant allele present in at least 1% of the population (1). Germline SNPs can be associated with the

risk and onset of diseases, including cancer (2). Such variants can also predict disease outcome and/or response to treatment, even without their direct association with the disorder (3). SNPs located in coding regions and regulatory gene elements are more likely to affect protein levels and function, and non-synonymous SNPs with a low degree of differentiation in the

¹Massachusetts General Hospital Cancer Center and Department of Medicine, Harvard Medical School, Boston, Massachusetts. ²Department of Environmental Health, Harvard School of Public Health, Harvard University, Boston, Massachusetts. ³Department of Epidemiology and Biostatistics, School of Public Health, Nanjing Medical University, Nanjing, Jiangsu, China. ⁴Pulmonary and Critical Care Unit, Massachusetts General Hospital, Harvard Medical School, Boston, Massachusetts.

Note: Supplementary data for this article are available at Cancer Discovery Online (<http://cancerdiscovery.aacrjournals.org/>).

Corresponding Author: Johnathan R. Whetstine, Department of Medicine, Massachusetts General Hospital Cancer Center, Harvard Medical School, Building 149, Room 7-213, 13th Street, Charlestown, MA 02129. Phone: 617-643-4347; Fax: 617-724-9648; E-mail: jwhetstine@hms.harvard.edu

doi: 10.1158/2159-8290.CD-14-1159

©2015 American Association for Cancer Research.

population are significantly more frequent in genes known to modulate diseases. Thus, these SNPs likely result in deleterious protein function and are of interest for medical research (4).

To date, little knowledge exists about how coding SNPs alter the function of chromatin-modifying enzymes (5). Importantly, emerging data on somatic mutations in cancer have identified these enzymes as critical cancer genes (5). For this reason, germline variants in these enzymes are likely determinants in disease susceptibility and therapeutic drug responses. Consistent with this notion, a coding SNP in the lysine demethylase gene *KDM4C* has recently been linked to breast cancer outcome (6). Therefore, understanding the molecular and biochemical roles of these enzymes and factoring in the impact SNPs have on their biology will be necessary to identify important disease biomarkers and provide insights into novel therapies or drug combinations.

In the present study, we describe the cellular and biochemical impact of a SNP in the coding region of the lysine demethylase gene *KDM4A*. *KDM4A* is a JmjC domain-containing lysine demethylase targeting H3K9me₃, H3K36me₃, and H1.4K26me₃ (7). Ubiquitination of *KDM4A* is a major regulatory mechanism for controlling the identified functions of this protein (8, 9). Consistent with the need to modulate *KDM4A* levels, tumors have been shown to have both gain and loss of *KDM4A* alleles. Although *KDM4A* overexpression and *KDM4A* copy gain have been shown to affect nuclear functions such as site-specific copy regulation (10), defined roles for *KDM4A* loss or decreased expression need additional exploration.

We have identified a coding SNP within *KDM4A* that results in the conversion of the glutamic acid at position 482 to alanine (E482A; referred to as SNP-A482). Consistent with this SNP having important biologic associations, we observe differential distribution across ethnic populations and poor outcome in patients with homozygous SNP-A482 non-small cell lung cancer (NSCLC). Furthermore, we demonstrate that SNP-A482 increases ubiquitination and protein turnover by increasing the interaction of *KDM4A* with the SKP1-Cul1-F-box (SCF) complex. An unbiased drug sensitivity screen of cells homozygous for SNP-A482 establishes an unprecedented link between *KDM4A* and inhibition of the mTOR pathway. In fact, mTOR inhibitors significantly reduce SNP-A482 protein levels when compared with wild-type (WT) *KDM4A*. Consistent with this observation, reduced *KDM4A* protein levels increase mTOR inhibitor sensitivity. Taken together, these findings report the first coding germline variant in a lysine demethylase that affects chemotherapeutic response, which identifies *KDM4A* as a potential candidate biomarker for mTOR inhibitor therapy.

RESULTS

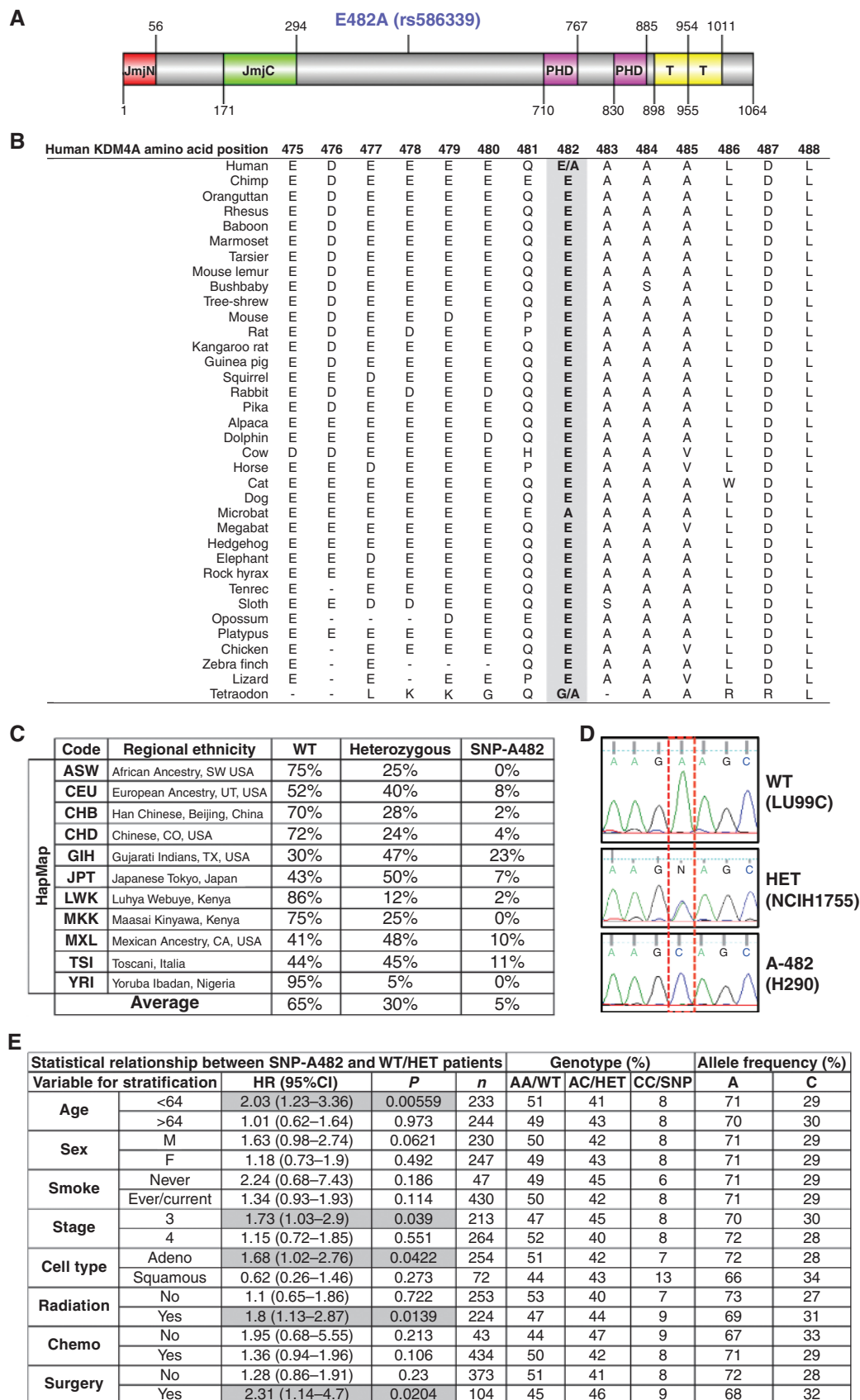
SNP-A482 Is Associated with Worse Outcome in Patients with NSCLC

Our laboratory has recently demonstrated that the lysine demethylase *KDM4A* is copy gained and lost in various cancers (10). Consistent with our studies, other groups have established that *KDM4A* protein levels are linked to cell proliferation, metastatic potential, and patient outcome for lung and bladder cancers (11, 12). Therefore, we evaluated whether there are genetic factors that could influence *KDM4A* protein levels and function. Specifically, we evaluated non-synonymous coding SNPs in *KDM4A* because they are more likely to alter protein function due to a change in an amino acid sequence (5). Our evaluation of the Database of Single Nucleotide Polymorphisms (dbSNP) identified only one coding SNP for *KDM4A* with reported allele frequencies.

KDM4A SNP rs586339A>C has a minor allele frequency of 0.238. The rs586339 SNP results in a single base substitution that leads to an amino acid substitution: E482 (GAA) to A482 (GCA). Therefore, we refer to this germline variant as SNP-A482 (Fig. 1A). We identified adenine “A” encoding E482 to be the major allele (referred to as WT throughout the text and figures) for two reasons: (i) this amino acid is conserved across species (Fig. 1B) and (ii) both the dbSNP and HapMap analysis reported “A” as the major allele. Upon evaluating the HapMap project, we observed different allelic frequencies across various ethnic populations (Fig. 1C; ref. 13), highlighting an ethnic diversity for this SNP. The average HapMap allelic frequency across all evaluated populations is 65% for homozygote for the major allele (WT), 30% for heterozygote, and 5% for homozygote for the minor allele (SNP-A482; Fig. 1C). The presence of the SNP in cell lines was confirmed using Sanger sequencing (Fig. 1D) and restriction fragment length polymorphism (not shown).

To further establish whether SNP-A482 had any disease associations, we evaluated a well-characterized cohort of patients with NSCLC (14, 15) and determined whether patients with homozygous *KDM4A* SNP-A482 NSCLC were associated with differential outcome based on various clinical parameters. Interestingly, NSCLC and non-NSCLC cohorts exhibited comparable allelic frequency, suggesting that there is no selection against the A482 allele in patients with NSCLC (Supplementary Fig. S1A). Patients that were homozygous for *KDM4A* SNP-A482 experienced an overall worse outcome, with borderline statistical significance ($P = 0.055$), and had significantly worse outcomes for certain late-stage patient parameters ($P < 0.05$, Fig. 1E and Supplementary Fig. S1B–S1F).

Figure 1. *KDM4A*SNP-A482 (rs586339) correlates with worse outcome in patients with NSCLC. **A**, schematic of the human *KDM4A* protein is shown with both the protein domains and the position of the coding SNP rs586339 (E482A). Jumonji (JmjN and JmjC), PHD, and Tudor (T) domains are represented. **B**, E482 is the conserved allele. The alignment of sequence surrounding E482A is shown for multiple species. **C**, HapMap frequencies for rs586339 are presented (August 2010 HapMap public release #28; ref. 13). ASW, African Ancestry in SW USA ($n = 57$); CEU, U.S. Utah residents with ancestry from northern and western Europe ($n = 113$); CHB, Han Chinese in Beijing, China ($n = 135$); CHD, Chinese in Metropolitan Denver, CO ($n = 109$); GIH, Gujarati Indians in Houston, TX ($n = 99$); JPT, Japanese in Tokyo, Japan ($n = 113$); LWK, Luhya in Webuye, Kenya ($n = 110$); MKK, Maasai in Kinyawa, Kenya ($n = 155$); MXL, Mexican Ancestry in Los Angeles, CA ($n = 58$); TSI, Toscani in Italia ($n = 102$); YRI, Yoruba in Ibadan, Nigeria ($n = 147$). **D**, representative *KDM4A* sequencing plots from three different lung cancer cell lines—homozygote wild-type (WT, GAA:GAA), heterozygote (HET, GAA:GCA), and homozygote SNP (A-482, GCA:GCA). **E**, *KDM4A* SNP-A482 stratification for patients with late-stage NSCLC. 95% CI, 95% confidence interval; P , the P value; n , the number of patients in each category; AA, the genotype for homozygote WT (E482); AC, the genotype for heterozygote; CC, the genotype for homozygote SNP (A482). Gray boxes, parameters with significance, including the data in Supplementary Fig. S1 (panels B–F). Frequency comparisons were tested using the χ^2 test, and HRs were calculated using a Cox model. Also see Supplementary Fig. S1.



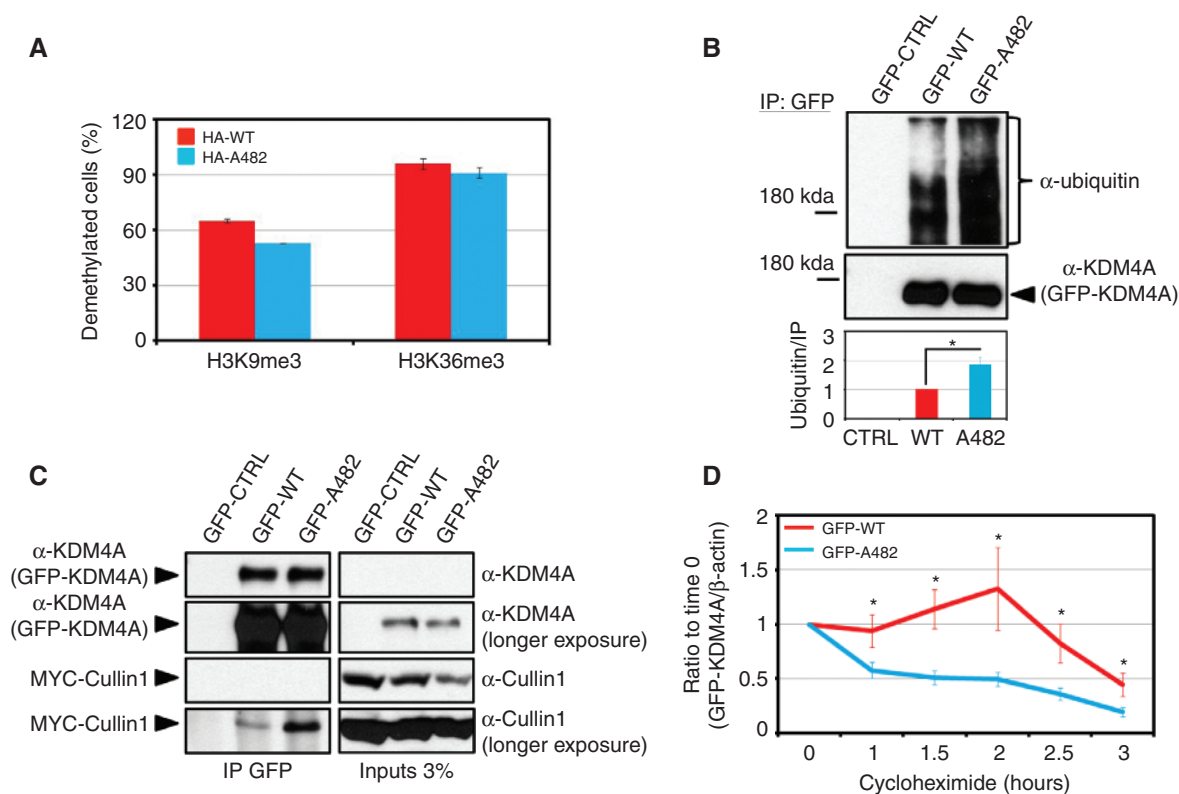


Figure 2. SNP-A482 promotes KDM4A ubiquitination and turnover. **A**, KDM4A WT and SNP-A482 comparably demethylate H3K36me3 and H3K9me3. 3xHA-KDM4A WT and 3xHA-KDM4A SNP-A482 were transfected into RPE cells, fixed, and stained with the indicated antibodies. This graph represents the average of two experiments. At least fifty cells were scored per experiment. **B**, KDM4A SNP-A482 exhibits a 2-fold greater ubiquitination than KDM4A WT. GFP-KDM4A WT and GFP-KDM4A SNP-A482 were transfected into HEK 293T cells before immunoprecipitation (IP) with a GFP antibody under denaturing conditions and immunoblotted with the indicated antibodies. Quantification was performed with ImageJ. The graph represents an average of five independent experiments that show the ratio of ubiquitin signal to the amount of immunoprecipitated protein. $P = 0.01$. **C**, GFP-A482 coimmunoprecipitates more MYC-Cullin1 than GFP-WT KDM4A. GFP-WT and GFP-A482 were transfected into HEK 293T cells before being immunoprecipitated with a GFP antibody and immunoblotted with the indicated antibodies. **D**, GFP-A482 has a shorter half-life than GFP-WT KDM4A. HEK 293T cells overexpressing GFP-WT or GFP-A482 were treated with cycloheximide and Western blotted. The y axis represents the ratio of GFP-tagged KDM4A relative to time 0, which was normalized to β -actin. The average of 16 independent experiments is shown. All error bars represent the SEM. P values were determined by a two-tailed Student t test; *, $P < 0.05$.

To further evaluate the predictive ability of SNP-A482 as a biomarker of survival and outcome, we performed time-dependent ROC curve analyses on five subgroups of patients with NSCLC (age < 64, adenocarcinoma, stage 3, with radiation therapy, and with surgery). In each subgroup, we compared the area under the curve of the model with SNP-A482 and clinical information (age, sex, smoking status) to the model with clinical information only. In general, the predictive model with SNP-A482 had a slightly better performance, with the caveat being the low heritability results in the predictive model being more limited (Supplementary Fig. S1G; ref. 16). Therefore, these data do not necessarily support the SNP-A482 serving as a biomarker alone; however, future studies containing larger sample sizes will help with the assessment of such a predictive model. These data do however highlight a disease association for SNP-A482 and support a rationale for exploring the impact SNP-A482 has on KDM4A.

SNP-A482 Results in Increased Ubiquitination and Turnover of KDM4A

We wanted to determine if there was a biochemical difference between KDM4A WT and KDM4A SNP-A482. Because

KDM4A is a histone demethylase (7), we determined whether KDM4A SNP-A482 had altered catalytic activity when compared with WT KDM4A *in vivo*. RPE cells transfected with either hemagglutinin (HA)-tagged WT or SNP-A482 KDM4A had similar H3K9me3 and H3K36me3 catalytic activities (Fig. 2A). However, SNP-A482 had an increase in higher molecular weight products when evaluated by Western blot (data not shown), which was demonstrated to be ubiquitination by immunoblotting for ubiquitin after denaturing GFP immunoprecipitation (Fig. 2B). Multiple replicate experiments indicated that there was a 2-fold increase in KDM4A SNP-A482 ubiquitination when the immunoprecipitation was normalized and compared with WT KDM4A (Fig. 2B, bottom; $P = 0.01$).

We and others have previously demonstrated that KDM4A is ubiquitinated by the SCF complex containing the E3 ligase Cullin1 (8, 9). Consistent with increased ubiquitination of KDM4A SNP-A482, KDM4A SNP-A482 coimmunoprecipitated more MYC-Cullin1, which reflects an increased association with the SCF complex (Fig. 2C). In addition, KDM4A SNP-A482 exhibited a shorter half-life when compared with KDM4A WT (1 hour, 38 minutes vs. 2 hours, 58 minutes, respectively; Fig. 2D). Taken together, these data demonstrate

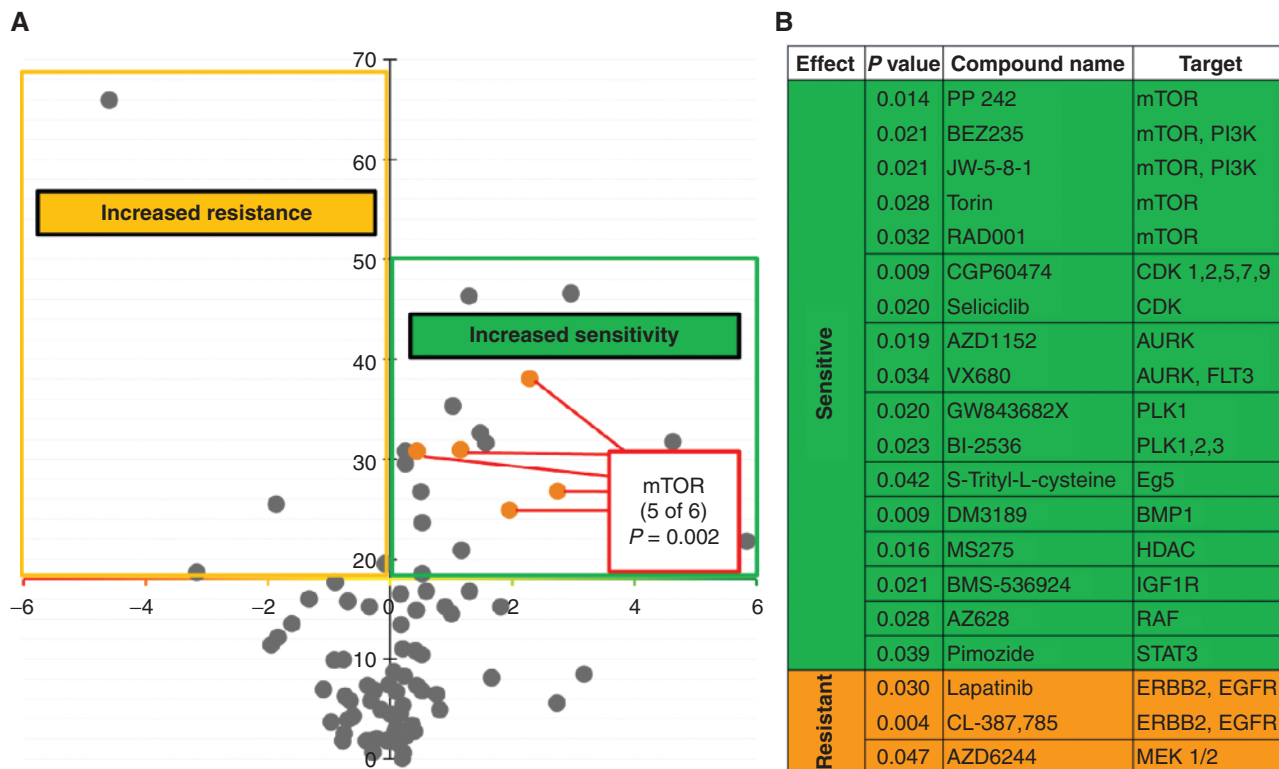


Figure 3. KDM4A SNP-A482 affects cellular sensitivity to specific drugs. **A**, volcano plot representing statistical significance (inverted Y axis) versus the effect of KDM4A SNP-A482 on drug sensitivity. Compounds above the X axis are statistically significant ($P < 0.05$). Eighty-six cell lines and eighty-seven compounds were used; the statistical significance of the enrichment for mTOR inhibitors in the group of drugs linked to the SNP status is indicated ($P = 0.002$). **B**, a list of compounds with statistically different sensitivity in **A**, their associated targets, and corresponding P values are shown. P values were calculated with the Fisher exact test. Also see Supplementary Fig. S2 and Supplementary Table S1.

that SNP-A482 results in altered KDM4A ubiquitination and contributes to changes in KDM4A protein stability.

KDM4A SNP-A482 Alters Chemotherapeutic Sensitivity in Lung Cancer Cell Lines

To determine whether there are differential roles between KDM4A WT and SNP-A482, we first assessed the impact of SNP-A482 on KDM4A-dependent phenotypes. Similar to WT KDM4A, SNP-A482 overexpression resulted in faster progression through S phase and promoted site-specific copy gains (data not shown). In a further attempt to resolve differences between the WT and SNP-A482-containing cells, we conducted an unbiased association study between 86 genotyped lung cancer cell lines (Supplementary Fig. S2A) and their corresponding drug sensitivities. These cell lines were treated with 87 preclinical and clinical compounds at three different drug concentrations (Supplementary Table S1). We compared the cell lines homozygous for the minor allele with the cell lines heterozygous and homozygous for the major allele. The results of the analysis are summarized as a volcano plot representing the statistical significance (inverted Y axis) versus the effect of KDM4A SNP-A482 on drug sensitivity (Fig. 3A). KDM4A SNP-A482 was significantly associated with altered drug response to 20 compounds: 17 compounds (green) were associated with increased drug sensitivity and three compounds (orange) were associated with increased

drug resistance (Fig. 3A and B). These compounds were then classified based on reported literature and known targets (Fig. 3B). The most striking enrichment was observed for mTOR inhibitors. Lung cancer cells homozygous for KDM4A SNP-A482 had increased sensitivity to five different mTOR/PI3K inhibitors ($P = 0.002$; Fig. 3A and B). Supplementary Fig. S2A shows that the different mTOR inhibitors have a consistent effect across each cell line used in our screen. This consistency is illustrated by looking at the relative sensitivity to each inhibitor obtained by median centering of the viability ratio values. Importantly, 10 of the 17 compounds that were associated with increased sensitivity in SNP-A482 homozygous cell lines are involved in targeting pathways related to mTOR/PI3K signaling (Supplementary Fig. S2B).

To further establish the specificity of the relationship between KDM4A SNP-A482 and mTOR inhibition, we examined the relationship between drug sensitivity and other SNPs within KDM4A (Supplementary Fig. S2C and S2D). We genotyped the lung cancer cell lines used in the initial screen for two additional KDM4A SNPs. We chose to study the noncoding SNP rs517191, which lacks significant association with overall outcome of patients with NSCLC, and the noncoding SNP rs6429632, for which the significant outcome associations in homozygous late-stage patients were not identical to that of KDM4A SNP-A482 [rs586339; Supplementary Fig. S2D]. Interestingly, only cell lines homozygous

for *KDM4A* SNP-A482 and not rs517191 or rs6429632 exhibited increased sensitivity to the majority of mTOR inhibitors compared with the cells heterozygous and homozygous for the major alleles (Supplementary Fig. S2E). These data suggest that the mTOR pathway directly or indirectly associates with SNP-A482.

mTOR Inhibition Reduces KDM4A Protein Levels

Because of the enrichment for mTOR inhibitor sensitivity in relation to SNP-A482, we further evaluated the biochemical relationship between *KDM4A* SNP-A482 and this class of compounds. Based on the observation that *KDM4A* SNP-A482 increases *KDM4A* ubiquitination and turnover (Fig. 2), we determined the impact that mTOR inhibition had on endogenous *KDM4A* levels in a heterozygous cell line (Fig. 4A–C). Consistent with mTOR inhibition affecting mRNA translation (17, 18), endogenous *KDM4A* protein levels were reduced during rapamycin treatment (Fig. 4A and B), whereas RNA levels were unchanged (Fig. 4C). Because *KDM4A* SNP-A482 has a faster half-life compared with *KDM4A* WT (Fig. 2D), we hypothesized that SNP-A482 protein levels would be lower than *KDM4A* WT protein levels in the presence of mTOR inhibitors. To test this hypothesis, we treated two cell lines of each of the *KDM4A* homozygous genotypes [i.e., homozygote SNP-A482 (Fig. 4D) or WT (Fig. 4E)] with rapamycin and analyzed endogenous *KDM4A* levels over time (Fig. 4D and E and Supplementary Fig. S3A). Indeed, H290 and RERF-LC-KJ cells, which are homozygous for *KDM4A* SNP-A482, exhibited reduced endogenous *KDM4A* protein levels upon mTOR inhibition (Fig. 4D), whereas LU99B and H2591 cells, which are homozygous for *KDM4A* WT, did not exhibit this phenotype (Fig. 4E and Supplementary Fig. S3A, compare blue line with red line, $P = 0.034$, significance for overall difference). To rule out the contribution of different genetic backgrounds in these cancer cell lines, we performed the same experiments within a single cell line that transiently overexpressed GFP-*KDM4A* WT or GFP-*KDM4A* SNP-A482. We observed the same phenotype in these cells (Supplementary Fig. S3B, compare blue line with red line, respectively; $P = 0.003$, significance for overall difference). Taken together, these data suggest that mTOR inhibition leads to a more pronounced decrease in SNP-A482 protein levels than WT *KDM4A*.

Reduced KDM4A Protein Levels Enhance Cell Sensitivity to mTOR Inhibitors

We hypothesized that the increased mTOR inhibitor sensitivity observed for *KDM4A* SNP-A482 cell lines was due at least in part to the stronger reduction in *KDM4A* levels upon mTOR inhibitor treatment. To test this hypothesis, *KDM4A* was depleted from cells using shRNAs, and cell proliferation was monitored during rapamycin treatment. Indeed, shRNAs directed against *KDM4A* further extended the already increased doubling time observed after rapamycin treatment (Fig. 4F and Supplementary Fig. S3C). To confirm this result, cells were depleted of *KDM4A* before treatment with the ATP-competitive mTOR inhibitor AZD8055 for 48 hours before cell proliferation, and viability was assessed using 3-[4,5-dimethylthiazol-2-yl]-2,5 diphenyl tetrazolium bromide (MTT) assays. Independent experiments demonstrated an increased sensitiv-

ity to mTOR inhibition upon *KDM4A* knockdown (Fig. 4G and Supplementary Fig. S3D; data not shown). Consistent with these observations, we most recently demonstrated that *KDM4A* interacts with translation initiation factors and modulates protein synthesis, which was enhanced with mTOR inhibition (19). Taken together, these data suggest that SNP-A482 status and *KDM4A* levels play an important role in sensitizing cells to mTOR inhibitors (Fig. 4H).

DISCUSSION

Personalized therapy is becoming more common in cancer treatment (20). For example, SNP status can be used to assess risk of disease or predict outcome and/or response to treatment and may also have a place in the subclassification of patients for optimal treatment delivery (2, 3). The ultimate goal of this approach is to utilize the genetic/biochemical properties of a target in certain cancer types and/or individuals to provide more effective treatment strategies. To achieve this goal, genetic and biochemical properties need to be established for genetic alterations linked to diseases.

To the best of our knowledge, this is the first report that identifies a coding SNP within a chromatin modifier with links to NSCLC outcome and drug response. These data are particularly important given that 85% of lung cancers are NSCLC, with 70% presenting as advanced disease, i.e., locally advanced IIIB or metastatic disease IV, and are not considered curable. The 5-year survival rates for these advanced NSCLC stages are 7% and 2%, respectively. Moreover, mTOR and PI3K inhibitors are being used to treat NSCLC (20, 21). Testing for multiple biomarkers to apply more targeted therapies is already considered to be the standard of care for lung cancer (20). Therefore, our study provides another possible option to stratify and possibly treat subgroups of patients with NSCLC.

We report that *KDM4A* SNP-A482 is linked to worse outcome in patients with NSCLC; however, the analyses suggest that this single variable is not a sufficient biomarker. Future studies with larger datasets are required to better clarify this possibility. The association with worse outcome in our data could reveal the fact that *KDM4A* levels or altered functions result in a benefit to certain tumors. For example, tumors with lower *KDM4A* protein levels have been shown to predict significantly worse overall survival (12). Interestingly, 20% of tumors assessed from The Cancer Genome Atlas present a copy loss of *KDM4A*, which correlated with a decrease in *KDM4A* RNA levels (10). Furthermore, reduced *KDM4A* protein levels are observed with cancer progression and metastasis (12). Therefore, tumors with SNP-A482 could possess an ability to more effectively reduce *KDM4A* levels. Another possibility is that because SNP-A482 is germline transmitted, the cells throughout the body could be the basis for the associated worse outcome. For example, patients could have impaired immune responses, increased toxicity to therapies, or altered tissue repair. For these reasons, analyses of additional datasets as well as prospective genetic studies evaluating the response of tumors and the individual to treatment as well as noted toxicities will be necessary to fully understand the impact of the SNP on patient outcome.

Because SNP-A482 and *KDM4A* depletion increased mTOR inhibitor sensitivity, we suspect that other cancer subtypes will also be good candidates for this genetic or

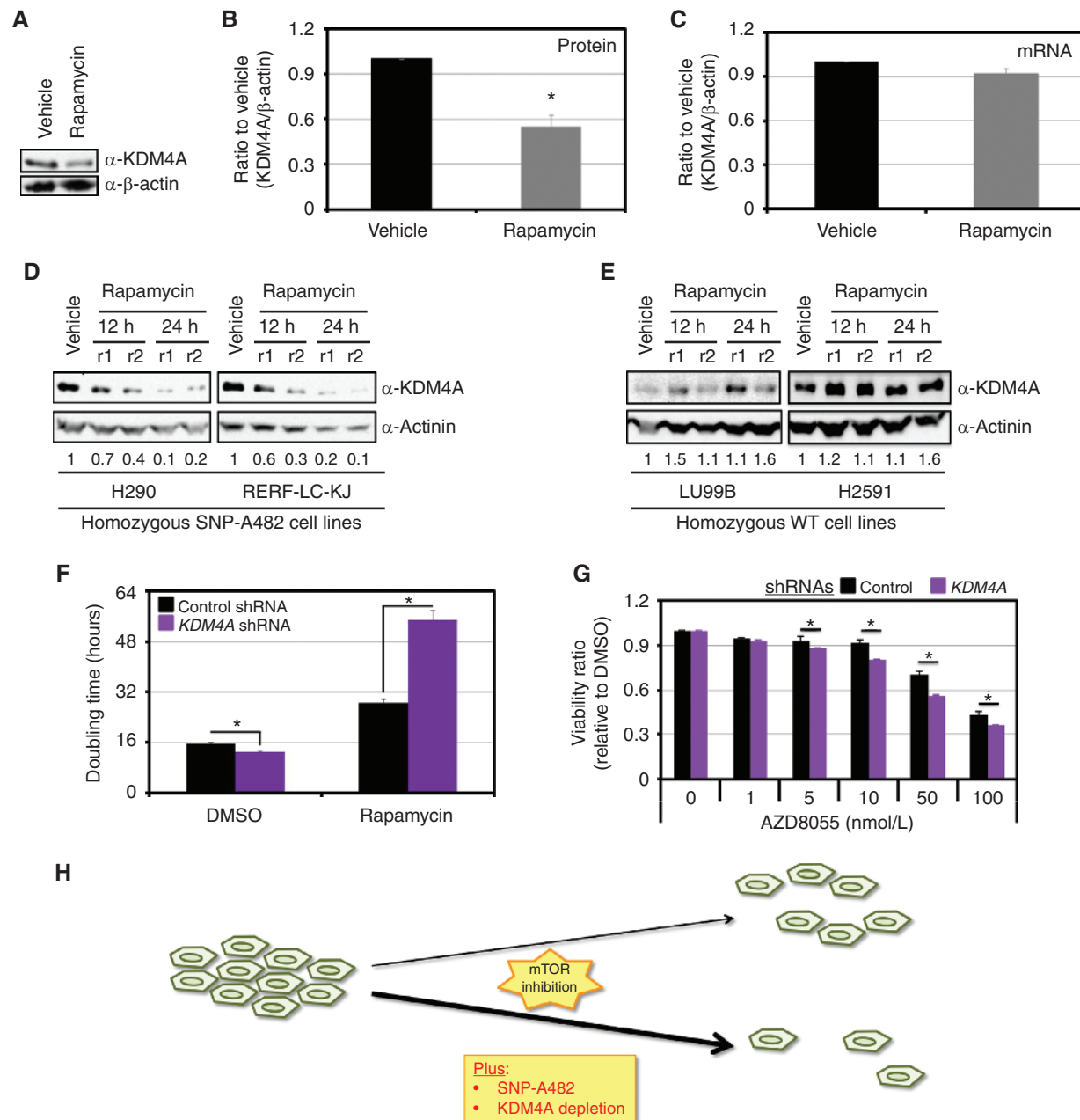


Figure 4. KDM4A levels affect cellular sensitivity to mTOR inhibitors. **A**, KDM4A protein levels decrease upon rapamycin treatment. HEK 293T cells were treated with 100 ng/mL of rapamycin for 24 hours. **B**, graphical representation of an average of three independent experiments from **A**. **C**, KDM4A RNA levels are stable upon rapamycin treatment. HEK 293T cells were treated with 100 ng/mL of rapamycin for 24 hours before RNA was harvested. An average of three independent quantitative RT-PCR experiments is represented. **D–E**, endogenous KDM4A SNP-A482 protein levels decrease more upon rapamycin treatment than WT KDM4A. Lung cell lines homozygous for KDM4A SNP-A482 (**D**; H290 and RERF-LC-KJ) or WT (**E**; LU99B and H2591) were treated with 100 ng/mL of rapamycin for 24 hours. Independent replicates (r1 and r2) are shown per time point. Quantification was performed with ImageJ. The numbers under the blots represent the ratio of the amount of KDM4A to the amount of Actinin, normalized to vehicle. **F**, HEK 293T cells transfected with three different shRNAs directed against KDM4A have increased sensitivity to rapamycin when compared with control vector-transfected cells. HEK 293T cells were seeded 24 hours after transfection and treated with 100 ng/mL of rapamycin 24 hours after seeding. The graphs represent the doubling time between 5 and 35 hours after rapamycin treatment. An average of three independent experiments is represented. **G**, HEK 293T cells transfected with shRNA 4A.6 are more sensitive to AZD8055 than cells transfected with the control vector. Cells were seeded 24 hours after the second shRNA transfection and were then treated with the indicated drugs and associated concentrations 24 hours later. Forty-eight hours after treatment, samples were analyzed by an MTT assay. The assays were normalized to a sample collected and assayed at the treatment time. The Y axis represents the viability ratio relative to DMSO. The average of three independent experiments is represented. **H**, model, KDM4A depletion of SNP-A482 enhanced the sensitivity to mTOR inhibitors. All error bars represent the SEM. *P* values were determined by a two-tailed Student *t* test; *, *P* < 0.05. Also see Supplementary Fig. S3.

chemical-based targeting in the future (Fig. 4H). For example, the mTOR inhibitor temsirolimus (CCI-779) is used for advanced refractory renal cell carcinoma (RCC; ref. 22). A phase II clinical trial presented an objective response rate for only 7% of patients with RCC (22). Interestingly, this proportion is similar to that observed for individuals homozygous for the rs586339 minor allele (*KDM4A* SNP-A482; Fig. 1C and Supplementary Fig. S1A). It would be interesting to determine whether response correlates with *KDM4A* SNP-A482 status in RCC.

In conclusion, we have now uncovered a genetic feature in *KDM4A* (SNP-A482) that could allow patient stratification and more effective treatment options for these individuals. Because the *KDM4A* allele is lost in certain tumors (10), these tumors could also be ideal candidates for mTOR-related chemotherapies. Overall, the current study highlights the fact that biochemical and cellular analyses of somatic and polymorphic variants within chromatin-modifying enzymes can identify associated signaling pathways and establish optimal chemotherapeutic targets in the future.

METHODS

Cell Culture and Drug Treatments

For tissue culture and generation of stable cell lines, see ref. 10. HEK 293T and RPE cells have been obtained from the ATCC, and no authentication has been done by the authors. All lung cell lines were sourced from commercial vendors. To exclude cross-contaminated or synonymous lines, a panel of 92 SNPs was profiled for each cell line (Sequenom), and a pairwise comparison score was calculated. In addition, we performed short tandem repeat (STR) analysis (AmpFlSTR Identifier; Applied Biosystems) and matched this to an existing STR profile generated by the providing repository. After initial expansion and STR analysis, each stock vial of cells was not propagated for more than 2 months. Rapamycin (LC Laboratories) and AZD8055 (Selleckchem) were used at indicated concentrations. Cycloheximide and MG132 were used as described in ref. 8.

Plasmids, shRNAs, and Transfections

Plasmid transfections were performed using X-tremeGENE 9 DNA transfection reagent (Roche) on 6×10^5 HEK 293T cells plated in 10-cm dishes 20 hours before transfection. The complexes were incubated with the cells in OptiMEM for 4 hours before being replaced by fresh media. Cells were harvested 48 to 72 hours after transfection. The transfected plasmids were as follows: pCS2-3xHA-KDM4A, pCS2-3xHA-KDM4A-E482A, pMSCV-GFP (10), pMSCV-GFP-KDM4A (10), pMSCV-GFP-KDM4A-E482A, pcDNA3-3xMYC-Cullin1 (8), pSUPER (10), pSUPER-4C (referred as 4A.2 throughout the figures; ref. 10), pLKO, pLKO-A06 (referred as 4A.6 throughout the figures), and pLKO-A10 (referred as 4A.10 throughout the figures). For the MTT assays, shRNAs were transfected twice 48 hours apart.

Western Blot Analysis

Western blot analyses were performed according to ref. 8.

Antibodies

The following antibodies were used: Actinin (Santa Cruz; sc-17829), Ubiquitin, *KDM4A*, Cullin 1, and β -actin, as described previously (8).

HapMap Frequencies

The HapMap frequencies are from the HapMap Public Release #28 (13).

Coimmunoprecipitation

The coimmunoprecipitation experiments were performed as described in ref. 8.

Catalytic Activity of *KDM4A* WT and SNP-A482

All immunofluorescence experiments were performed as in ref. 10. Fifty cells were scored per replicate.

Patient Outcome

For complete methods, see ref. 15. *P* values have been calculated based on a recessive model with unadjusted covariates. The time-dependent ROC curve analyses have been done as described in ref. 16. The patient studies were conducted in accordance with the Declaration of Helsinki. The Institutional Review Board of the Massachusetts General Hospital approved the studies, and all patients provided informed consent.

Drug Screen

A panel of 86 cell lines was used in a high-throughput viability screen as described previously (23). The cell lines were randomly selected from a collection of 160 lung cancer cell lines available at Massachusetts General Hospital (MGH), and based on the mutational data available, they appear to be representative of NSCLC lines in general and capture major mutational events described for this cancer at the expected frequency. All mutational data available are provided in Supplementary Table S2. Additional details are available in ref. 24. The compounds were targeted agents mostly at late stage of clinical or preclinical development, selected based on therapeutic relevance of the drugs themselves or of the targets for compounds not clinically tested. They cover a broad range of targets not restricted to the PI3K pathway, including CDK, Aurora, proteasome, EGFR, SRC, IGF1R, and MEK. The compounds cover over 50 different nominal targets with some redundancy toward the most clinically relevant targets. The full list of drugs and their primary target is provided as Supplementary Table S3.

Cells were seeded in 96-well plates at approximately 15% confluency in medium with 5% FBS and penicillin/streptavidin. The optimal cell number for each cell line was determined to ensure that each was in growth phase at the end of the assay. After overnight incubation, cells were treated with three concentrations of each compound in triplicate (10-fold dilution series) using liquid handling robotics, and then returned to the incubator for assay at a 72-hour time point. Cells were fixed in 4% formaldehyde for 30 minutes and then stained with 1 μ mol/L of the fluorescent nucleic acid stain Syto60 (Invitrogen) for 1 hour. Quantitation of fluorescent signal intensity was performed using a fluorescent plate reader at excitation and emission wavelengths of 630/695 nm. The mean of triplicate values for each drug concentration was compared with untreated wells, and a viability ratio was calculated.

The statistical association between drug sensitivity and *KDM4A* SNP-A482 status was tested using a series of Fisher exact tests designed to capture the differential drug effect across the full range of viability observed: For these tests, the cell lines were designated as *KDM4A* SNP-A482 positive if they were homozygous for the minor allele and compared with heterozygous and homozygous major allele cell lines grouped together. For each drug and concentration used, the cell lines were rank ordered from most to least sensitive and a contingency table was built by designating the top 5% sensitive cell lines as "sensitive" and the rest as "resistant." The result of the Fisher exact test for this threshold of sensitivity was recorded, and the procedure was repeated using as a sensitivity threshold the 10th percentile to the 75th percentile by five percentiles increment. The minimum *P* value for a given drug across the three concentrations tested is reported. The drug effect is the difference between the mean viability of *KDM4A* SNP-A482 homozygous cell lines and the mean

viability of the other cell lines tested at the concentration matching the reported Fisher exact test *P* value. The statistical significance of the enrichment for mTOR inhibitors in the group of drugs associated with the presence of the minor allele *KDM4A* SNP-A482 was tested using a Fisher exact test with five mTOR inhibitors and 15 other drugs statistically linked to *KDM4A* SNP-A482 status versus one mTOR inhibitor and 66 other drugs not statistically linked to *KDM4A* SNP-A482 status.

Monitored Cell Proliferation Assay

Twenty-four hours after transfection, 1×10^4 HEK 293T cells were seeded per well of a 96-well plate, and then treated after 24 hours. Cell proliferation was monitored with an xCELLigence system (Roche; ref. 25).

MTT Assays

MTT assays were performed following supplier's instructions from the Cell Proliferation Kit I (MTT) from Roche. For shRNA experiments, after two subsequent shRNA transfections, cells were seeded in 96-well plates before being treated 24 hours later. Briefly, 1×10^4 cells were seeded per well of a 96-well plate and grown for 24 hours before treatment. Forty-eight hours later, cells were assayed. We determined sensitivity by subtracting the background from the absorbance.

Statistical Analysis

All error bars represent SEM. Half-lives were calculated using a polynomial trend line (8). *P* values were determined by a two-tailed Student *t* test or a two-way ANOVA when noted; * represents *P* < 0.05. For the analyses of patients with NSCLC, frequency comparisons were tested using the χ^2 test. HRs and the significances of the association were calculated using a Cox model. The Kaplan–Meier method was used to estimate the survival curves. For the drug screen, *P* values were calculated with the Fisher exact test.

Disclosure of Potential Conflicts of Interest

J.R. Whetstine is a consultant/advisory board member for QSonica. No potential conflicts of interest were disclosed by the other authors.

Authors' Contributions

Conception and design: C. Van Rechem, D.C. Christiani, J.R. Whetstine
Development of methodology: C. Van Rechem

Acquisition of data (provided animals, acquired and managed patients, provided facilities, etc.): C. Van Rechem, J.C. Black, P. Greninger, Y. Zhao, C. Donado, D.C. Christiani, C.H. Benes

Analysis and interpretation of data (e.g., statistical analysis, biostatistics, computational analysis): C. Van Rechem, J.C. Black, P. Greninger, Y. Zhao, P.d. Burrowes, D.C. Christiani, C.H. Benes, J.R. Whetstine

Writing, review, and/or revision of the manuscript: C. Van Rechem, J.C. Black, B. Ladd, D.C. Christiani, C.H. Benes, J.R. Whetstine

Administrative, technical, or material support (i.e., reporting or organizing data, constructing databases): P. Greninger, Y. Zhao, B. Ladd, D.C. Christiani, J.R. Whetstine

Study supervision: J.R. Whetstine

Acknowledgments

The authors thank Drs. Elnaz Atabakhsh and Yongyue Wei as well as Kelly Biette for their comments and suggestions.

Grant Support

The studies conducted in this article were funded by an American Cancer Society Basic Scholar Grant, an MGH Proton Beam Federal Share Grant (CA059267), and NIH R01GM097360 (to J.R. Whetstine); NIH (NCI) grant 5R01CA92824 (to D.C. Christiani); and

NIH grant U54 HG006097 (to C.H. Benes). J.R. Whetstine is the Tepper Family MGH Research Scholar and a Leukemia and Lymphoma Society Scholar, as well as a recipient of the American Lung Association Lung Cancer Discovery Award. A postdoctoral fellowship was provided by the Fund for Medical Discovery to C. Van Rechem. C. Van Rechem is the 2014 Skacel Family Marsha Rivkin Center for Ovarian Cancer Research Scholar. This research was supported in part by a grant from the Marsha Rivkin Center for Ovarian Cancer Research. J.C. Black was a fellow of The Jane Coffin Childs Memorial Fund for Medical Research and is supported by an MGH ECOR Testeson Postdoctoral Fellowship. This investigation has also been aided by a grant from The Jane Coffin Childs Memorial Fund for Medical Research.

The costs of publication of this article were defrayed in part by the payment of page charges. This article must therefore be hereby marked *advertisement* in accordance with 18 U.S.C. Section 1734 solely to indicate this fact.

Received October 1, 2014; revised December 8, 2014; accepted December 19, 2014; published OnlineFirst January 6, 2015.

REFERENCES

- Brookes AJ. The essence of SNPs. *Gene* 1999;234:177–86.
- Zeron-Medina J, Wang X, Repapi E, Campbell MR, Su D, Castro-Giner F, et al. A polymorphic p53 response element in KIT ligand influences cancer risk and has undergone natural selection. *Cell* 2013;155:410–22.
- Lee JC, Espeli M, Anderson CA, Linterman MA, Pocock JM, Williams NJ, et al. Human SNP links differential outcomes in inflammatory and infectious disease to a FOXO3-regulated pathway. *Cell* 2013;155:57–69.
- Barreiro LB, Laval G, Quach H, Patin E, Quintana-Murci L. Natural selection has driven population differentiation in modern humans. *Nat Genet* 2008;40:340–5.
- Van Rechem C, Whetstine JR. Examining the impact of gene variants on histone lysine methylation. *Biochim Biophys Acta* 2014;1839:1463–76.
- Hong Q, Yu S, Yang Y, Liu G, Shao Z. A polymorphism in JMJD2C alters the cleavage by caspase-3 and the prognosis of human breast cancer. *Oncotarget* 2014;5:4779–87.
- Black JC, Van Rechem C, Whetstine JR. Histone lysine methylation dynamics: establishment, regulation, and biological impact. *Mol Cell* 2012;48:491–507.
- Van Rechem C, Black JC, Abbas T, Allen A, Rinehart CA, Yuan GC, et al. The SKP1-Cul1-F-box and leucine-rich repeat protein 4 (SCF-FbxL4) ubiquitin ligase regulates lysine demethylase 4A (KDM4A)/Jumonji domain-containing 2A (JMJD2A) protein. *J Biol Chem* 2011;286:30462–70.
- Tan MK, Lim HJ, Harper JW. SCFFBXO22 Regulates Histone H3 Lysine 9 and 36 methylation levels by targeting histone demethylase KDM4A for ubiquitin-mediated proteasomal degradation. *Mol Cell Biol* 2011;31:3687–99.
- Black JC, Manning AL, Van Rechem C, Kim J, Ladd B, Cho J, et al. KDM4A lysine demethylase induces site-specific copy gain and rereplication of regions amplified in tumors. *Cell* 2013;154:541–55.
- Kogure M, Takawa M, Cho HS, Toyokawa G, Hayashi K, Tsunoda T, et al. Deregulation of the histone demethylase JMJD2A is involved in human carcinogenesis through regulation of the G(1)/S transition. *Cancer Lett* 2013;336:76–84.
- Kauffman EC, Robinson BD, Downes MJ, Powell LG, Lee MM, Scherr DS, et al. Role of androgen receptor and associated lysine-demethylase coregulators, LSD1 and JMJD2A, in localized and advanced human bladder cancer. *Mol Carcinog* 2011;50:931–44.
- Altshuler DM, Gibbs RA, Peltonen L, Dermitzakis E, Schaffner SF, Yu F, et al. Integrating common and rare genetic variation in diverse human populations. *Nature* 2010;467:52–8.
- Huang YT, Heist RS, Chirieac LR, Lin X, Skaug V, Zienoldiny S, et al. Genome-wide analysis of survival in early-stage non-small-cell lung cancer. *J Clin Oncol* 2009;27:2660–7.

15. Heist RS, Zhai R, Liu G, Zhou W, Lin X, Su L, et al. VEGF polymorphisms and survival in early-stage non-small-cell lung cancer. *J Clin Oncol* 2008;26:856–62.
16. Chambless LE, Diao G. Estimation of time-dependent area under the ROC curve for long-term risk prediction. *Stat Med* 2006;25:3474–86.
17. Bjornsti MA, Houghton PJ. The TOR pathway: a target for cancer therapy. *Nat RevCancer* 2004;4:335–48.
18. Populo H, Lopes JM, Soares P. The mTOR signalling pathway in human cancer. *Int J Mol Sci* 2012;13:1886–918.
19. Van Rechem C, Black JC, Boukhali M, Aryee MJ, Gräslund S, Haas W, et al. Lysine demethylase KDM4A associates with translation machinery and regulates protein synthesis. *Cancer Discov* 2015;5:255–63.
20. Cagle PT, Allen TC, Olsen RJ. Lung cancer biomarkers: present status and future developments. *Arch Pathol Lab Med* 2013;137:1191–8.
21. Gridelli C, Maione P, Rossi A. The potential role of mTOR inhibitors in non-small cell lung cancer. *Oncologist* 2008;13:139–47.
22. Atkins MB, Hidalgo M, Stadler WM, Logan TF, Dutcher JP, Hudes GR, et al. Randomized phase II study of multiple dose levels of CCI-779, a novel mammalian target of rapamycin kinase inhibitor, in patients with advanced refractory renal cell carcinoma. *J Clin Oncol* 2004;22:909–18.
23. McDermott U, Sharma SV, Settleman J. High-throughput lung cancer cell line screening for genotype-correlated sensitivity to an EGFR kinase inhibitor. *Methods Enzymol* 2008;438:331–41.
24. Garnett MJ, Edelman EJ, Heidorn SJ, Greenman CD, Dastur A, Lau KW, et al. Systematic identification of genomic markers of drug sensitivity in cancer cells. *Nature* 2012;483:570–5.
25. Vistejnova L, Dvorakova J, Hasova M, Muthny T, Velebny V, Soucek K, et al. The comparison of impedance-based method of cell proliferation monitoring with commonly used metabolic-based techniques. *Neuro Endocrinol Lett* 2009;30:121–7.

CANCER DISCOVERY

A Coding Single-Nucleotide Polymorphism in Lysine Demethylase *KDM4A* Associates with Increased Sensitivity to mTOR Inhibitors

Capucine Van Rechem, Joshua C. Black, Patricia Greninger, et al.

Cancer Discovery 2015;5:245-254. Published OnlineFirst January 6, 2015.

Updated version	Access the most recent version of this article at: doi: 10.1158/2159-8290.CD-14-1159
Supplementary Material	Access the most recent supplemental material at: http://cancerdiscovery.aacrjournals.org/content/suppl/2015/01/27/2159-8290.CD-14-1159.DC1.html

Cited Articles	This article cites by 25 articles, 7 of which you can access for free at: http://cancerdiscovery.aacrjournals.org/content/5/3/245.full.html#ref-list-1
-----------------------	--

Citing articles	This article has been cited by 2 HighWire-hosted articles. Access the articles at: http://cancerdiscovery.aacrjournals.org/content/5/3/245.full.html#related-urls
------------------------	---

E-mail alerts	Sign up to receive free email-alerts related to this article or journal.
----------------------	--

Reprints and Subscriptions	To order reprints of this article or to subscribe to the journal, contact the AACR Publications Department at pubs@aacr.org .
-----------------------------------	--

Permissions	To request permission to re-use all or part of this article, contact the AACR Publications Department at permissions@aacr.org .
--------------------	---